USGS
science for a changing world

Local Tsunami Hazards in the Pacific Northwest from Cascadia Subduction Zone Earthquakes

Professional Paper 1661-B

U.S. Department of the Interior
U.S. Geological Survey

Earthquake Hazards of the Pacific Northwest Costal and Marine Regions

Robert Kayen, Editor

Local Tsunami Hazards in the Pacific Northwest from Cascadia Subduction Zone Earthquakes

By Eric L. Geist

In estimating the tsunami hazards for the Pacific Northwest posed by major earthquakes along the Cascadia subduction zone, it is important to identify uncertainties associated with tsunami generation and their effect on near-shore tsunami amplitudes. Earthquake parameters, such as width of rupture and distribution of slip, cause significant variability in local tsunami estimates. These uncertainties are best incorporated in a probabilistic analysis of tsunami hazards.

Professional Paper 1661-B

U.S. Department of the Interior
U.S. Geological Survey

U.S. Department of the Interior
Gale A. Norton, Secretary

U.S. Geological Survey
Charles G. Groat, Director

U.S. Geological Survey, Reston, Virginia: 2005

For sale by U.S. Geological Survey Information Services
Box 25286, Denver Federal Center
Denver, CO 80225

This report and any updates to it are available online at:
http://pubs.usgs.gov/pp/pp1661b

For additional information write to:
U.S. Geological Survey
Box 25046, Mail Stop 421, Denver Federal Center
Denver, CO 80225-0046

Additional USGS publications can be found at:
http://geology.usgs.gov/products.html

For more information about the USGS and its products:
Telephone: 1–888–ASK–USGS (1–888–275–8747)
World Wide Web: http://www.usgs.gov/

Cataloging-in-publication data are on file with the Library of Congress (URL http://www.loc.gov/).

Produced in the Western Region, Menlo Park, California
Manuscript approved for publication, January 3, 2005
Text edited by Peter Stauffer
Layout and design by Susan Mayfield and Judy Weathers

FRONT COVER
Computer simulation of tsunami wavefield 20 minutes after a hypothetical magnitude 7.8 earthquake on the Cascadia subduction zone. Topography and wave heights vertically exaggerated at different scales to illustrate wavefield.

Contents

Figures

Local Tsunami Hazards in the Pacific Northwest from Cascadia Subduction Zone Earthquakes

By Eric L. Geist[1]

Abstract

Since the mid-1980s, there has been accumulating geologic evidence of large local tsunamis generated by earthquakes along the Cascadia subduction zone off the Pacific Northwest. Information from recent geophysical and geological investigations constrains the potential rupture-zone geometry and average repeat time of interplate thrust earthquakes. Based on this information, tsunami hazard maps have been prepared for coastal communities in the Pacific Northwest using sophisticated numerical models to simulate tsunami propagation and inundation. In this study, sources of uncertainty in tsunami hazard calculations are described and a probabilistic hazard analysis for tsunamis, similar to probabilistic seismic hazard analysis (PSHA), is outlined. Though probabilistic tsunami hazard analysis (PTHA) shares many similarities with PSHA, there are specific issues unique to tsunami hazards that need to be accounted for in the probability calculations. For example, the possibility of rupture along splay faults from the Cascadia interplate thrust have a large effect on tsunami generation, but a relatively small impact on peak ground accelerations onshore. The largest sources of uncertainty include the average slip and downdip extent of rupture. Also, it is demonstrated that significant variations in nearshore tsunami amplitude are caused by uncertainty in slip distribution patterns. Correct identification of uncertainties related to tsunami generation and propagation is critical in performing the probability calculations. PTHA has the potential to provide an improved technique for evaluating local tsunami hazards in the Pacific Northwest and elsewhere.

Introduction

Before the mid-1980s, the hazard posed by local tsunamis to the Pacific Northwest coast received minimal attention, primarily because of that region's lack of destructive local tsunamis in recorded history. Comparative studies of the world's subduction zones by Heaton and Kanamori (1984) and later studies by Heaton and Hartzell (1986, 1989) led to the recognition of the seismic potential for interplate thrust events and associated tsunamis along the Cascadia subduction zone. More recent paleoseismologic studies have focused on the last large interplate thrust event in 1700 C.E. and recurrence intervals from previous events (Atwater, 1987, 1992; Atwater and Hemphill-Haley, 1997; Kelsey and others, 2002; Witter and others, 2003). Turbidites along the Oregon-Washington continental margin also are thought to record the occurrence of great Cascadia earthquakes, of which 13 have been recorded since the Mount Mazama eruption (approximately 7.7 ka.; Adams, 1996; Goldfinger and others, 2003). Independent corroboration of the 1700 C.E. event comes from the investigation of Satake and others (1996) and Satake and others (2003), who analyzed tsunami records in Japan and deduced that a far-field tsunami that struck Japan most likely came from a large magnitude earthquake along the Cascadia subduction zone. These geologic investigations prompt a closer look at the hazards from local tsunamis in the Pacific Northwest.

Evidence that the interplate thrust is currently locked and not slipping freely comes from the analysis of geodetic data (Savage and others, 1991; Hyndman and Wang, 1995; Oleskevich and others, 1999; Wang and others, 2003). Significant secular uplift rates (approx. 4 mm/yr, Savage and others, 1991) and horizontal axes of contraction subparallel to the plate convergence direction are consistent with deformation patterns from an interseismic period in which the interplate thrust is locked (Savage and others, 1991; Dragert and others, 1994; Mitchell and others, 1994; Hyndman and Wang, 1995; Wang and others, 2003). Hyndman and Wang (1995) and Oleskevich and others (1999) further constrain the width of the locked zone from thermal modeling of the subduction zone, validated from heat flow measurements (fig. 1). As a possible analog to the Cascadia subduction zone, Mazzotti and others (2000) analyze data from a dense GPS network in Japan and determine that the Nankai and Japan-West Kurile subduction zones were fully locked during the period of measurement. Placing this result in the context of the abundant seismic history of Japan led Mazotti and others (2000) to conclude that heterogeneous slip distribution patterns from past earthquakes are in marked contrast to homogeneous interseismic loading and that a significant part of the elastic strain along the interplate thrust may be released through slow earthquakes or post-seismic slip. (See Dragert and others, 2001, for analysis of a recent slow event along the deeper part of the Cascadia subduction zone.) A thorough review of seismicity and geodetic

[1] Menlo Park, California

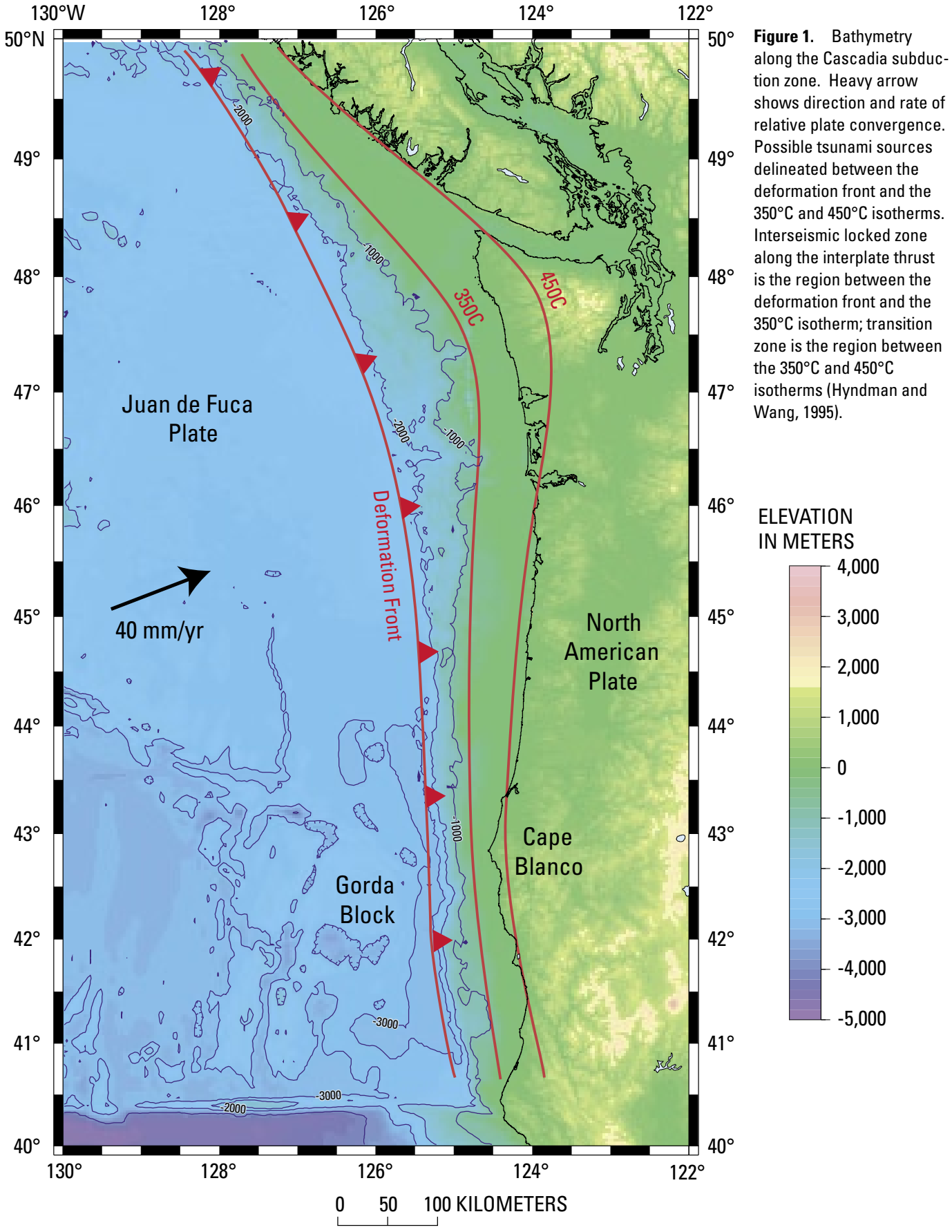

Figure 1. Bathymetry along the Cascadia subduction zone. Heavy arrow shows direction and rate of relative plate convergence. Possible tsunami sources delineated between the deformation front and the 350°C and 450°C isotherms. Interseismic locked zone along the interplate thrust is the region between the deformation front and the 350°C isotherm; transition zone is the region between the 350°C and 450°C isotherms (Hyndman and Wang, 1995).

data, interpretation, and arguments for and against seismic and aseismic subduction, is given by Rogers and others (1996).

Quantification of the local tsunami hazard typically relies on the analysis of past instrumentally recorded events. Unfortunately, there are no recordings of tsunamigenic events along the Cascadia subduction zone, except for the 1992 Cape Mendocino earthquake at the southernmost extent of the subduction zone (Oppenheimer and others, 1993; González and others, 1995). Seismicity in the region is primarily located along a well-defined Benioff zone and within the North American Plate; no earthquakes of any magnitude on the interplate thrust of the Washington-Oregon segment of the Cascadia subduction zone have been recorded since 1970 (Ludwin and others, 1991). In this respect, the Cascadia subduction zone is unlike any other subduction zone around the world in which distinctive long-term seismicity patterns are evident (Kanamori, 1981; Pérez and Scholz, 1997). The lack of interplate seismicity along the Cascadia subduction zone obviously impedes quantitative estimation of ground shaking, as well as of tsunami generation from major interplate thrust earthquakes.

Previous studies have estimated tsunami hazards in the Pacific Northwest by considering a limited number of different earthquake scenarios (Hebenstreit and Murty, 1989; Ng and others, 1990; Whitmore, 1993; Priest and others, 1997, 2000; Preuss and Hebenstreit, 1998; see also review by Mofjeld and others, 1999). Among these studies, several different earthquake locations and magnitude were considered, but rupture complexity in terms of nonuniform slip, nonplanar faulting, and heterogeneous elastic structure was not. Geist and Yoshioka (1996) examined the effect that variations in earthquake source parameters have on tsunamis generated along the Cascadia subduction zone, still from the standpoint of uniform slip, however. In later papers, Geist and Dmowska (1999) and Geist (2002) emphasize the fundamental importance that distributed slip has on tsunami generation. In particular, these papers stress that the initial tsunami wavefield calculated using uniform-slip models will underestimate both the amplitude and leading-wave steepness of the local tsunami (fig. 2*A*). In producing inundation maps for Yaquina Bay, Oregon, Priest and others (1997, 2000) present a thorough review of possible variations of regional source parameters and their effect on tsunami generation. A number of rupture scenarios were considered in the development of these inundation maps, including variations in slip by way of prescribing asperities with higher slip than the surrounding rupture area (specified by uniform slip). Tsunami inundation maps for the coast of southern Washington were prepared using a similar source model for a Cascadia interplate thrust earthquake (Walsh and others, 2000) and using a simplified source by Preuss and Hebenstreit (1998). In the present paper, sources of uncertainty in assessing tsunami hazards in the Pacific Northwest are described and a probabilistic tsunami hazard analysis (PTHA) is outlined. Though PTHA can be based on the same earthquake source models as used for the National Seismic Hazard maps (Frankel and others, 1996, 2002), issues specific to tsunami generation and propagation are described that need to be addressed when calculating tsunami probabilities.

Interplate Thrust Earthquakes

As mentioned in the introduction, potential interplate thrust events along the Cascadia margin are difficult to define, owing to the lack of historical precedents. Paleoseismologic data do suggest that slip along the interplate thrust is accommodated by large ($M > 8$) earthquakes, though not all necessarily rupture the entire subduction zone (Adams, 1996; Atwater and Hemphill-Haley, 1997; Kelsey and others, 2002; Goldfinger and others, 2003; Witter and others, 2003). In this respect, the pattern of rupture occurrence appears more like that of characteristic earthquakes than a Gutenberg-Richter distribution of earthquake magnitudes (Wesnousky, 1994). From the standpoint of constructing a worst-case scenario, it is unclear whether tsunami earthquakes (that is, earthquakes that generate much larger tsunami amplitudes in comparison to other tsunamigenic earthquakes for a given magnitude; Kanamori, 1972; Kanamori and Kikuchi, 1993; Polet and Kanamori, 2000) may occur along the Cascadia subduction zone that could generate local tsunamis larger than the one derived from the 1700 event. An appropriate approach is to follow the two earthquake recurrence scenarios considered by Frankel and others (1996) and Frankel and others (2002) for the Cascadia subduction zone: (1) a single M 9 event that ruptures the entire subduction zone every 500 years on average and (2) a series of M 8.3 events (ruptures 250 km long) that collectively fill the entire subduction zone every 500 years.

The locked zone that controls interseismic deformation (Savage and others, 1991; Hyndman and Wang, 1995; Flück and others, 1997; Oleskevich and others, 1999; Wang and others, 2003) provides basic information with which we can constrain earthquake rupture (fig. 1). These authors generally define a locked seismogenic zone from approximately the base of the continental slope to the 350°C isotherm and a transition zone where seismic and aseismic slip could occur between the 350°C and 450°C isotherms (fig. 1). Scholz (1990) indicates that large earthquakes frequently transgress upper and lower stability boundaries (updip to the sea floor or downdip into the transition zone). The upper stability boundary, if it exists, is difficult to define (Flück and others, 1997). For a large earthquake initiating at depth, it is likely that rupture will break through to the sea floor, as suggested by Rudnicki and Wu (1995) from the point of view of crack mechanics and as suggested by Kanamori and Kikuchi (1993) for some tsunami earthquakes. Dmowska and Kostrov (1973) and Rudnicki and Wu (1995) demonstrate that a rupture that extends to the traction-free sea floor will be associated with substantially large slip for a given earthquake moment in comparison to a shallow imbedded rupture (that is, one that does not reach the sea floor). Geist and Dmowska (1999) show, however, that the tsunami size will not increase proportionally with slip for a sea-floor rupturing event over an imbedded event, owing to characteristic changes in the slip distribution between the two types of events. For either an imbedded or a sea-floor rupture, the initial tsunami wave profile calculated using heterogeneous

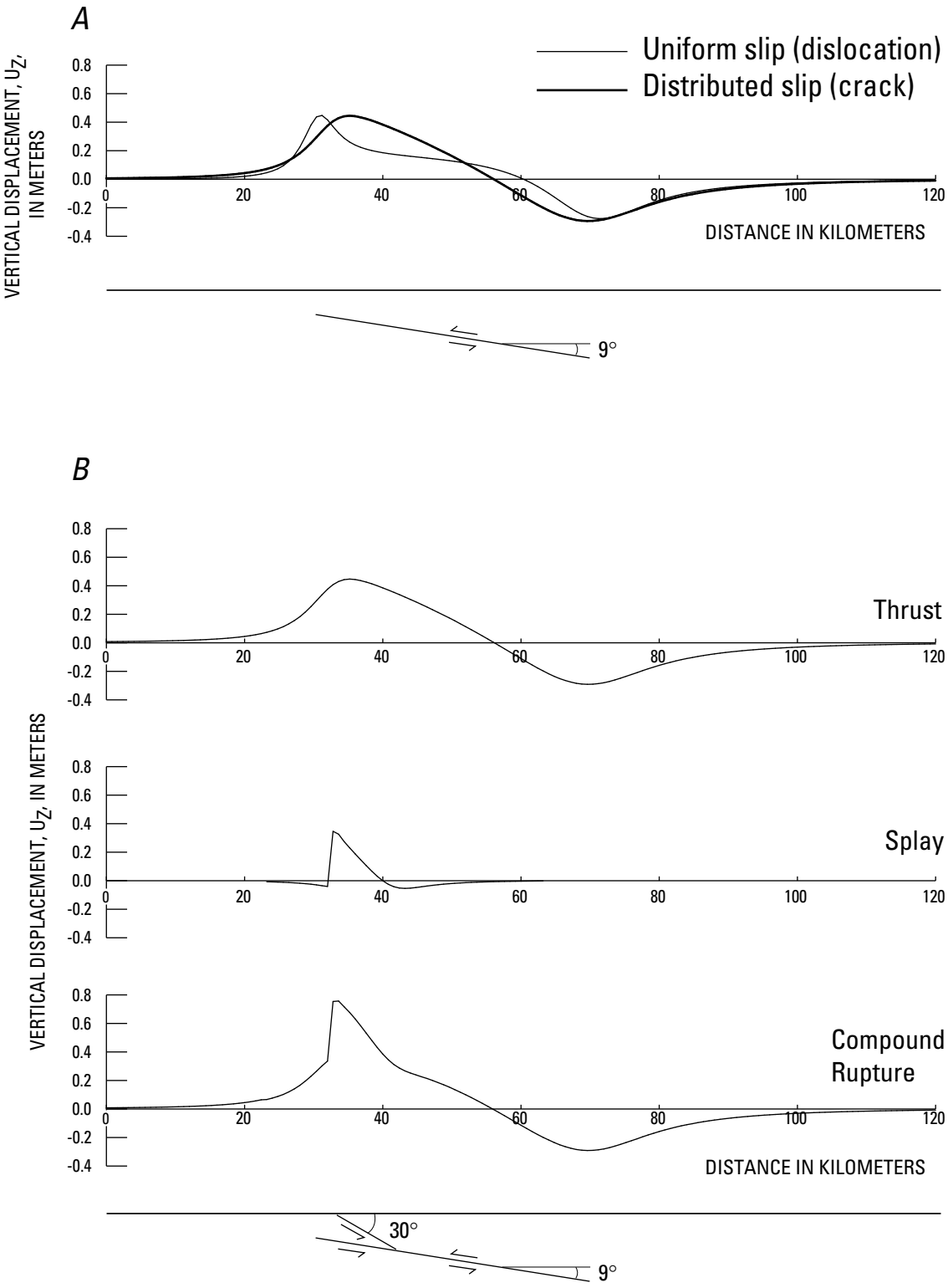

Figure 2. Initial tsunami wave profiles from crack models (Geist and Dmowska, 1999). *A*, Comparison of initial wave profiles from a crack model (thick line) and a uniform slip dislocation model (thin line). Geometry of imbedded thrust fault rupture shown below. Rupture is 40 km wide, with an average of 1.16 m of slip. *B*, Effect of splay faulting on tsunami generation. Vertical displacement field for a compound rupture is calculated by superimposing the displacement fields for the decollement fault modeled as an imbedded crack and the splay fault modeled as a surface-rupture crack. Geometry of compound thrust fault rupture shown below. Rupture on main thrust is 40 km wide, with an average of 1.16 m of slip.

slip will be significantly different from the profile calculated using standard, uniform slip dislocation models (fig. 2*A*).

The potential interplate rupture zone along the Cascadia margin is significantly narrower compared to other subduction zones (Zhang and Schwartz, 1992; Tichelaar and Ruff, 1993; Flück and others, 1997; Oleskevich and others, 1999; Wang and others, 2003). The exceptionally high aspect ratio (rupture length : width ≅ 10:1) for the largest earthquake that could occur on the Cascadia subduction zone (Hyndman and Wang, 1995) is significantly larger than observed aspect ratios from other subduction zones (Geller, 1976; for example, the aspect ratio of the 1960 Chile earthquake is approximately 4:1). Recent work by Nielsen and others (2000) demonstrates the effects that rate-and-state friction parameters as well as rupture geometry have on rupture dynamics and periodicity. They indicate that two rupture regimes are present: (1) a cracklike regime with periodic to quasi-periodic events that rupture the entire fault and (2) a self-healing regime in which rupture propagates by self-healing pulses that exhibit strong dynamic complexity (see also Madariaga and others, 1998; Zheng and Rice, 1998). Furthermore, Nielsen and others (2000) indicate that as the aspect ratio of the rupture increases, the rupture regime crosses over from cracklike to self-healing. Large aspect ratios exhibit strong dynamic complexity (that is, strongly heterogeneous slip with regard to tsunami generation) and aperiodic recurrence intervals, according to these modeling studies.

Earthquakes with higher than expected tsunami excitation in Cascadia would include nonplanar rupture along seaward-vergent splay faults from the interplate thrust (fig. 2*B*). Fukao (1979) originally proposed this type of mechanism to explain tsunami earthquakes. Observations of vertical displacement following the 1964 Great Alaska earthquake by Plafker (1965) provide evidence for secondary rupture along splay faults during a major subduction zone earthquake. For a given seismic moment, slip on high-angle splay faults results in higher amounts of vertical displacement in comparison to lower angle interplate thrust events (Geist, 1999; Cummins and Kaneda, 2000). Both seaward-vergent and landward-vergent splay faults are imaged along the Cascadia subduction zone (MacKay and others, 1992), though only compound events involving interplate thrust and seaward-vergent splays are likely to result in increased tsunami amplitudes (Geist and Yoshioka, 1996). Instead of using simple elastic dislocations as in Geist and Yoshioka (1996), a slip distribution is used in this study that considers the decollement fault as an imbedded crack and the high-angle splay fault as a surface-rupture crack, using the expressions of Dmowska and Kostrov (1973). Vertical displacement in figure 2*B* is calculated as described in Geist and Dmowska (1999). For the position of the splay fault relative to the decollement as shown in figure 2*B*, peak vertical displacement is enhanced. The central question, however, is whether updip rupture along the decollement can propagate to a splay fault. This question has been addressed using a static analysis (Jeyakumaran and Keer, 1994) and, more recently, dynamic simulations (Aochi and others, 2000; Kame and others, 2003). In future studies, heterogeneous slip distributions, optimally derived from dynamic rupture simulations, such as Aochi and others (2000), or from seismic inversion results, should be used to accurately simulate the tsunami wavefield derived from compound rupture involving splay faults.

Other tsunami source parameters unique to tsunami earthquakes, such as low shear modulus/high slip, shallow rupture depth, and deep water in the source region, can result in increased tsunami excitation for an earthquake of a given seismic moment (Geist and Dmowska, 1999; Geist and Bilek, 2001). It is difficult to assess the likelihood of tsunami earthquake occurrence for the Cascadia subduction zone. Because of the elevated thermal regime, the region of frictional instability (that is, the region for potential rupture) is much shallower in Cascadia than in other subduction zones (Hyndman and Wang, 1995; Oleskevich and others, 1999). Whether or not rupture would transgress the upper frictional stability transition and break to the sea floor, producing a tsunami earthquake (see Kanamori and Kikuchi, 1993; Geist and Dmowska, 1999), is unclear (see also discussion by Priest and others, 1997). Because the zone of potential rupture is shallow within the solid earth and in relatively deep water, tsunami generation is more effective along the Cascadia subduction zone in comparison to other subduction zones for an earthquake of a given magnitude.

Tsunami Physics

Physics of Tsunami Generation, Propagation, and Runup

Before describing the uncertainties in tsunami hazard analysis and the probabilistic method, a summary of how tsunamis are generated by earthquakes and how tsunami waves propagate is given in this section. For a more complete review of tsunami physics, the reader is referred to Kajiura (1963), Carrier (1971), Mei (1983), Geist (1999), and Satake (2002).

Tsunamis are generated by earthquakes through the transfer of large-scale elastic deformation associated with earthquake rupture to potential energy within the water column. In most cases, the initial tsunami amplitude wavefield mimics the static, coseismic vertical displacement field associated with the earthquake. In regions of steep bathymetry, Tanioka and Satake (1996) demonstrate that the horizontal displacement field from an earthquake also contributes to the vertical displacement of the water column. Calculation of coseismic displacement field (u_k) is derived from expressions relating the slip of a dislocation over surface Σ imbedded in an elastic medium. The general definition of dislocation is meant in this case, where relative displacement is arbitrary along the rupture zone (Somigliana dislocation, Rybicki, 1986). The particular case of a Volterra dislocation is one where the relative displacement or slip (Δu_i) is constant. Volterra dislocations, most often considered in calculating coseismic displacement and expressions for specific cases (e.g., Mode I, II, and III frac-

tures, Okada, 1985), are derived from the general formulation for Volterra dislocations of Steketee (1958):

$$u_k = \frac{1}{8\pi\mu} \iint_{\Sigma} \Delta u_i \omega_{ij}^k \nu_j d\Sigma \quad ij = 1,2,3 \tag{1}$$

where, μ is the shear modulus, ω represents the static elastic Green's functions, and ν represents the unit surface-normal vectors.

Whereas the characterization of earthquake rupture using a single Volterra (uniform slip) dislocation or several Volterra dislocations that span the width of the rupture zone is common in tsunami modeling (for example, Imamura and others, 1995; Satake and Tanioka, 1995; Geist and Yoshioka, 1996; Piatanesi and others, 1996), Geist and Dmowska (1999) demonstrate the fundamental importance that distributed slip has on tsunami generation. As originally discussed by Freund and Barnett (1976) and later by Rudnicki and Wu (1995), the assumption of uniform slip implies that deformation is concentrated at the edges of rupture. In contrast, variable slip in the dip direction for a dip-slip fault will concentrate deformation near the center of the rupture zone and will result in substantially higher vertical displacements and therefore higher initial tsunami amplitudes in comparison to a uniform-slip rupture of identical seismic moment (Geist and Dmowska, 1999). Rupture in subduction-zone earthquakes is inherently complex, as indicated from seismic inversion results (Beck and Ruff, 1989; Thatcher, 1990), leading Geist (2002) to adapt a fractal source model of subduction-zone earthquake rupture to estimate the range of local tsunami amplitudes possible for a given earthquake. Stemming from a lack of knowledge of fault plane and rupture heterogeneity, simple dislocation models have been proposed for Cascadia subduction zone earthquakes (Hebenstreit and Murty, 1989; Whitmore, 1993; Flück and others, 1997). It should be recognized, however, that because dip variations in slip are not accounted for, these models may underestimate coseismic vertical displacement that controls initial tsunami amplitude.

Once generated, tsunamis propagate outward from the source region and behave according to shallow-water wave theory (inviscid), since tsunami wavelength is typically much greater than ocean depths. The shallow-water wave equations, neglecting bottom friction, are

$$\begin{aligned} &\frac{\partial(\eta + h)}{\partial t} + \nabla\bullet[\mathbf{v}(\eta + h)] = 0 \quad \text{Continuity Equation} \\ &\frac{\partial \mathbf{v}}{\partial t} + (\mathbf{v}\bullet\nabla)\mathbf{v} + g\ \eta\ \nabla = 0 \qquad \text{Momentum Equation} \end{aligned} \tag{2}$$

where h is the water depth, η is wave elevation, and $\mathbf{v}$ is the depth-averaged horizontal vector velocity field. For a broad range of periods (400 s < T < 10,000 s) in which the shallow-water wave equations are applicable, the phase velocity is given by $c = \sqrt{gh}$ (Ward, 1980). In water depths greater than ~50 m (Shuto, 1991), the shallow-water wave equations can be approximated by the linear long-wave equations:

$$\begin{aligned} &\frac{\partial(\eta + h)}{\partial t} + \nabla\bullet(h\mathbf{v}) = 0 \quad \text{Continuity Equation} \\ &\frac{\partial \mathbf{v}}{\partial t} + g\nabla\eta = 0 \qquad \text{Momentum Equation} \end{aligned} \tag{3}$$

Wave dynamics become increasingly more complicated as tsunamis approach shore. Because modeling tsunami runup involves moving boundary conditions and often turbulent flow, it has been difficult to devise a robust procedure that would be applicable to realistic shoreline geometries, even though theoretical treatments have been derived by, for example, Carrier and Greenspan (1958). Recently, however, there has been considerable effort toward the development of runup and overland flow models (Antunes do Carmo and Sebra-Santos, 1996; Sato, 1996; Johnsgard and Pedersen, 1997; Titov and Synolakis, 1998). Of note, Titov and Synolakis (1998) have developed a procedure where the nonlinear shallow-water wave equations (2) are split so that two-dimensional runup can be computed. In addition, coseismic subsidence and strong tidal fluctuations that can occur in the Pacific Northwest (Mofjeld and others, 1997) affect tsunami inundation patterns. Continued research in the area of tsunami runup will be critical for the development of accurate tsunami hazard maps.

Propagation Phenomena along the Pacific Northwest Continental Margin

Tsunamis generated by Cascadia interplate thrust earthquakes will be significantly affected by propagation over the broad continental shelf. Using high-order wave theory, Shibata (1983) demonstrates that frequency dispersion can have a significant effect on the local tsunamis propagating across continental shelves. Other studies indicate that the incidence angle, period, and shelf slope have a strong influence on reflection and transmission at the shelf break and coastline (Abe and Ishii, 1980; Carrier and Noiseux, 1983; Koshimura and others, 1999).

Tide gauge records of the 1992 Cape Mendocino tsunami demonstrated that edge waves can be excited along the Pacific Northwest coast (González and others, 1995). Edge waves are trapped coastal waves that occur in distinct modes, with an exponential amplitude decay away from shore. Ishii and Abe (1980) show how edge-wave excitation is dependent on continental margin geometry. Fujima and others (2000) demonstrate that when a tsunami source is close to the coastline (that is, a local tsunami), the gravest mode of edge waves is generated. For this type of edge wave, Fujima and others (2000) note that while a single edge-wave phase may not have a large amplitude (in comparison to the direct arrival), resonance and interference can cause locally high amplitudes at certain locations. As noted by González and others (1995), because the phase and group velocities for edge waves are much slower than nontrapped modes, large-amplitude arrivals at coastal observation points oblique to the source region

can occur much later than the first arrival (see Carrier, 1995). González and others (1995) emphasize that accurate tsunami assessments and forecasts need to account for the excitation of edge waves, particularly in the Pacific Northwest.

Framework for a Local Tsunami Hazard Assessment

Adaptation of Seismic Hazard Assessment Methods

Tsunami hazards in the past have primarily been assessed using deterministic methods. Typically, this involves the calculation of runup and inundation from (1) an incident design wave, not directly linked to a source model, (2) a designated maximum credible earthquake, or (3) a series of source scenarios as, for example, employed by Priest and others (1997). Probabilistic methods of hazard assessment have an advantage over deterministic methods by including measures of uncertainty and of the likelihood of the event occurring, often with the specification of risk-tolerance factor. Probabilistic methods have been used for analyzing the hazard from distant tsunamis based on historical data (for example, Houston and others, 1977) and simple seismological models (Lin and Tung, 1982; Rikitake and Aida, 1988). In a series of recent studies, probabilistic methods for tsunami hazard assessment are discussed for earthquakes, asteroid impacts, and landslides (Ward, 2000; Ward and Asphaug, 2000; and Ward, 2001, respectively). As formulated by Ward (2000), the Poissonian probability that a tsunami at a particular location along a coastline ($\mathbf{r}$) will exceed a particular risk tolerance (a_0) over a given time interval (T) is given by

$$P(\mathbf{r},T,a_0) = 1 - e^{-N(\mathbf{r},a_0)T} \quad (4)$$

where N is a total rate of exceedance integrated over all possible source locations and parameter space.

A probabilistic method for assessing tsunami hazards can be developed based on a similar method that has been in use for assessing the ground-motion hazard from earthquakes termed probabilistic seismic hazard analysis (PSHA). PSHA can be thought of in three steps: (1) specification of seismic sources; (2) calculation of ground motion using an empirical formula termed the attenuation relationship; and (3) calculation of the probabilities. Details of the PSHA method are described by Cornell (1968), National Research Council (1988), Ward (1994), Senior Seismic Hazard Analysis Committee (1997), and Anderson and Brune (1999). The PSHA method is instrumental in producing the National Seismic Hazard Maps (Frankel and others, 1996, 2002). For an analogous analysis of tsunami hazards (probabilistic tsunami hazard analysis, PTHA), the same specifications of the source (location, magnitude, and average repeat time) can be used as in PSHA. In calculating rate term (N) in equation 4 where empirical attenuation relationships are used in PSHA, Ward (2000) indicates that model-based relationships can instead be used for PTHA based on tsunami-generation and wave theory and the known bathymetry of the world's oceans. In applying this method for tsunamis produced by asteroid impact, Ward and Asphaug (2000) present the results of the probabilistic calculations in terms of the probability that a specific site (for example, San Francisco) can expect a wave of a specific height (for example, 5 m) over a given time period from the present (for example, 1,000 years). A similar probabilistic analysis is performed for potential submarine landslides in Ward (2001). Below, the sources of uncertainty specific to local tsunamis generated by Cascadia subduction zone earthquakes are discussed, as well as how these uncertainties may be incorporated into probabilistic calculations.

Sources of Uncertainty in Probabilistic Calculations

A convenient classification of the sources of uncertainty follows the evolution of the tsunami through three stages—generation, propagation, and runup. The least amount of uncertainty is associated with the propagation calculations, in which the hydrodynamics are relatively simple. The primary component of uncertainty, in this case, is errors in the bathymetry. The hydrodynamics of runup, in contrast, are much more complex, involving bottom friction, overland flow, and, in the case of breaking waves, turbulent behavior. To model these effects accurately, detailed bathymetry and topography are needed, but these are often difficult to obtain in the coastal zone. The uncertainty associated with runup is analogous to the uncertainty associated with site effects in PSHA. Uncertainty related to tsunami generation includes the pattern of occurrence for subduction-zone earthquakes (one M 9 earthquake or a series of M 8.3 earthquakes, as discussed previously) and the downdip extent of rupture. Both of these issues are addressed by Frankel and others (2002). Uncertainty in the shear modulus of rocks in the subduction zone may also be important in determining the amount of average slip from an earthquake of a given seismic moment (Geist and Bilek, 2001). Uncertainty in the average repeat time of these earthquakes is addressed in paleoseismological studies (see, particularly, Adams, 1996; Atwater and Hemphill-Haley, 1997; Goldfinger and others, 2003; and Witter and others, 2003). Variability in recurrence intervals indicated by these authors suggest the need for a conditional probability model such as the Brownian passage-time model proposed and applied to Cascadia events by Ellsworth and others (1999). In this paper, attention is drawn to the uncertainty of source parameters, including rupture geometry and slip distribution patterns.

To determine the possible range of tsunami amplitudes that arise from slip variations during rupture, we first need to bracket or isolate the calculations from other sources of uncertainty listed above. To exclude the uncertainty associated

with the hydrodynamics of runup, propagation calculations are stopped at the 50-m isobath. What is analyzed, in this case, is termed the peak nearshore tsunami amplitude (PNTA) as in Geist (2002). For the source specifications, a M 8.8-9.0 earthquake with geometric and average slip parameters indicated by Satake and others (2003) is analyzed. To explain the tsunami observations in Japan from the 1700 Cascadia earthquake, Satake and others (2003) consider six source scenarios: three long ruptures that span the length of the Cascadia subduction zone and three ruptures of less than 500 km in length (labeled "Short-North," "Short-Central," and "Short-South"). The three long ruptures include "Long-Narrow," in which full slip is imposed downdip to the 350°C isotherm (fig. 1) and then linearly decreasing to zero at the 450°C isotherm; "Long-Splayed," in which a splay fault (fig. 2) is invoked; and "Long-Wide," in which uniform slip is imposed downdip to the 450°C isotherm. Results from their tsunami modeling indicate that the Long-Narrow and Long-Splayed source scenarios best fit the tsunami data in Japan and the paleoseismic data in Cascadia. Wang and others (2003) suggest, on the basis of analogous events along the Nankai subduction zone in Japan, that coseismic rupture occurs within the locked zone and linearly decreases to zero at half the width of their wide effective transition zone. Rather than using uniform slip downdip to the 350°C isotherm, as in past studies, this paper uses the stochastic source model of Geist (2002) to produce a suite of slip-distribution patterns as described below. Two ruputure geometries are analyzed: (1) rupture down to the 450°C isotherm, as in the Long-Wide model of Satake and others (2003), and (2) rupture down to the 350°C isotherm, as in the Long-Narrow model of Satake and others (2003), except that slip does not continue into the transition zone.

For a given rupture location and geometry, the stochastic source model produces a wide range of slip-distribution patterns that are consistent with the high-frequency falloff observed in the far-field seismic displacement spectrum denoted by $\omega^{-\gamma}$, as well as the *b*-value in aftershock sequences (Hanks, 1979; Andrews, 1980; Frankel, 1991; Herrero and Bernard, 1994; Tsai, 1997). The $\omega^{-\gamma}$ spectral falloff is caused by self-similar variations in initial stress or stress drop (Hanks, 1979; Huang and Turcotte, 1988). The corresponding slip distribution follows a fractal scaling relationship in which the fractal exponent is linked to γ (Tsai, 1997). Hartzell and Heaton (1985) and Polet and Kanamori (2000) indicate that the spectral falloff exponent for subduction zone earthquakes ranges between $1.0 \leq \gamma \leq 2.6$. Polet and Kanamori (2000) indicate that γ is consistent within a given region and that there does not appear to be a difference in γ between tsunami earthquakes and typical subduction zone earthquakes for a given region. Because we have no information of the characteristic spectral decay for Cascadia subduction zone events, a radial-wavenumber slip spectrum that falls off as k^{-2} is used that corresponds to the generic ω^{-2} model of Aki (1967). The phase of the slip spectrum is randomized to produce slip-distribution patterns characterized by a single region of moment release or multiple subevents. In this example, each rupture has a nearly identical seismic moment ($M_w = 9.0$). Further details of the method are given by Geist (2002).

For a given slip-distribution and rupture geometry, the tsunami wavefield is calculated using a standard leap-frog finite-difference form of the linear long-wave equations (3). A computationally efficient threshold-type model is used to model tsunami propagation for a large number of sources, in which peak nearshore tsunami amplitude (PNTA) is calculated at the shallowest water depth where the linear long-wave equations are valid (approximately 50 m, Shuto, 1991; 20 m used in Preuss and Hebenstreit, 1998). The grid spacing in the finite-difference calculations is 1.3 km and the time step is 4.5 seconds. The wave history is modeled for the first 1.5 hours; tests indicate that longer times do not significantly effect the average or extreme values of the PNTA.

The variations in PNTA parallel to the Pacific Northwest coast are first calculated using 100 different slip-distribution patterns and a geometry similar to the Long-Wide model of Satake and others (2003) (rupture area shown in light blue in figure 3). In addition to the average (red) and maximum and minimum (blue) PNTA values along the coast, also shown in figure 3 are PNTA histograms for selected locations. These histograms illustrate the high degree of scatter (measured by the coefficient of variation) and complex distribution of PNTA values resulting from the 100 model runs. For all runs using the stochastic model, the average amount of slip for a rupture is thought to be consistent with tsunami heights in Japan (Satake and others, 2003) and coseismic subsidence (Leonard and others, 2004) from the 1700 C.E. event. For the first case, the average slip varies between 11.2 and 12.8 m ($M_w = 9.0$), consistent with the results of Sakate and others (2003) for conservative tsunami heights in Japan (labeled "Low" tsunami heights). The resulting subsidence along the coast is approximately 1.5 to 3 m (depending on the slip distribution), which is slightly higher than what is estimated by Leonard and others (2004) from paleoseismic evidence in coastal marshes. In comparison to previous models of local tsunamis in Cascadia (Hebenstreit and Murty, 1989; Whitmore, 1993), the average tsunami amplitudes using the Long-Wide model are similar in the northern part of the subduction zone (approx. 4-8 m) and slightly higher in the southern part of the subduction zone, where the downdip width narrows (approx. 8-13 m). Comparing the results in this study at specific sites where previous inundation models have been formulated, the range in tsunami amplitude offshore Grays Harbor, Washington (2-7 m) is slightly lower compared to the offshore amplitudes predicted by Preuss and Hebenstreit (1998) (7-8 m). The range in tsunami amplitude at Yaquina Bay, Oregon (5.5-10.5 m) encompasses the runup predicted by Priest and others (1997) using an asperity source model (8.5 m). It should be noted that the finer grid size used by Priest and others (1997) results in better resolution of small-scale changes in alongshore tsunami amplitude than the regional model used in this study.

A second series of simulations was performed by limiting the slip downdip to the 350°C isotherm. The geometry is similar to the Long-Narrow rupture of Satake and others

(2003), except that in this case slip does not continue into the transition zone (rupture area shown in light blue in figure 4). It is important to note that in all cases the slip distribution is completely described by the stochastic source model; no ad hoc taper of slip with depth is imposed as in the studies of Priest and others (1997, 2000) and Satake and others (2003). The average amount of slip used in this case is 12.5–14.5 m, such that M_w = 8.8-8.9 for all 100 earthquakes. This amount of slip is consistent with Satake and others (2003) "Medium" tsunami heights in Japan and with paleoseismologic estimates of subsidence from the 1700 C.E. event. Because slip is concentrated at shallow depth beneath the sea floor and under relatively deep water, it produces a larger tsunami compared to the Long-Wide model (fig. 4). This rupture may be similar to what would be expected from a tsunami earthquake (Satake and Tanioka, 1999; Geist and Bilek, 2001; Bilek and Lay, 2002). Whether or not such large amounts of slip can be sustained shallow in the subduction zone and over a long fault length is not known. Although as much as 10 m of slip was estimated from the M_w =7.7 1992 Nicaragua tsunami earthquake (Ihmlé, 1996), tsunami earthquakes greater than M_w ~8.2 are unknown (Bilek and Lay, 2002).

The low-wavenumber scaling of the stochastic model is prescribed by the mean slip along the fault ($\overline{\Delta u}$)

$$\overline{\Delta u}(k) = C\frac{\Delta\sigma}{\mu}L_0 \quad k < 1L_0 \tag{5}$$

as given by Herrero and Bernard (1994), where $\Delta\sigma$ is the mean stress drop, μ is the shear modulus, L_0 is the characteristic rupture length, and C is a geometric factor. In the scenarios presented here, for convenience, these parameters were constrained by the average slip from the last earthquake (1700 C.E.). Although there are scaling laws among these low-order earthquake source parameters (Kanamori and Anderson, 1975; Geller, 1976; Wyss, 1979; Romanowicz and Rundle, 1993; Scholz, 1994; Wells and Coppersmith, 1994) there exists significant uncertainty in these empirical relations as indicated by the observed data, especially when tsunami earthquakes are considered (see Geist, 1999, for mean slip versus M_0 specific to subduction-zone earthquakes). Comparison of results from the simulations shown in figures 3 and 4 demonstrate that, in addition to uncertainty in the amount of average slip, there are large effects on nearshore tsunami amplitudes from variations in slip-distribution patterns and the downdip limit of rupture.

In addition to the source effects described above, spikes in the PNTA distribution are caused by localized amplification near headlands and promontories and can be termed site response. Because of refraction, bathymetric promontories will focus tsunami energy, whereas embayments (in the absence of resonance) will defocus tsunami energy. Similar site responses along the outer coast were obtained in previous modeling studies (Hebenstreit and Murty, 1989; Whitmore, 1993; Preuss and Hebenstreit, 1998), though the site response depends in part on the propagation path from the source to the shoreline (Geist, 2002). For example, there is a significant difference in site response near latitude 43° N between the two sets of simulations (figs. 3, 4) that results from the interplay between propagation path difference and a complex coastal response from the irregular bathymetry near Cape Blanco. Because tsunami propagation calculations were not made past the 50 m isobath, more detailed hydrodynamic studies are needed to compute the nearshore site response, particularly in estuaries and inland waterways as in Priest and others (1997).

Incorporating Uncertainty into Probabilistic Calculations

In probabilistic hazard analyses, uncertainties are classified as either being epistemic or aleatory. Toro and others (1997) define epistemic uncertainty as uncertainty "that is due to incomplete knowledge and data about the physics of the earthquake process. In principle, epistemic uncertainty can be reduced by the collection of additional information." Toro and others (1997) define aleatory uncertainty as uncertainty "that is inherent to the unpredictable nature of future events. It represents unique details of source, path, and site response that cannot be quantified before the earthquake occurs. Aleatory uncertainty cannot be reduced by collection of additional information. One may be able, however, to obtain better estimates of the aleatory uncertainty by using additional data." Although in some cases it can be difficult to determine whether a source of uncertainty is epistemic or aleatory (Panel on Seismic Hazard Evaluation, 1997), Anderson and Brune (1999) assert that the results of PSHA are critically dependent on correct classification of uncertainties. In the calculations of exceedance probabilities (equation 4), aleatory uncertainty is incorporated into the calculation of the rate term $N(r,a_0)$. In contrast, epistemic probabilities result in distinct hazard curves $P(r,T,a_0)$ that are often aggregated using logic trees (see, for example, National Research Council, 1988; Cramer and others, 1996).

Following the definitions given by Toro and others (1997) and the examples given by Anderson and Brune (1999), it is clear that most uncertainties associated with tsunami propagation calculations are epistemic. That is, the collection of bathymetry of higher accuracy and resolution than is presently available will lead to a reduction in the uncertainty associated with the propagation path. Similarly, the availability of high-resolution nearshore bathymetry and topography reduces the uncertainty associated with wave amplification and runup. However, turbulent behavior, in particular with breaking waves, can be considered as a source of aleatory uncertainty, because the collection of additional data does not necessarily improve our estimate of turbulent dynamics. Though turbulent dynamics is a topic of active research, in most modeling applications it is treated approximately using eddy viscosity terms in a turbulent closure scheme (for example, Mellor and Yamada, 1974; Blumberg and Mellor, 1987; Sato, 1996).

For the seismic hazard maps, uncertainties associated with the earthquake source (specifically, the characteristic magnitude) are divided into both epistemic and aleatory components

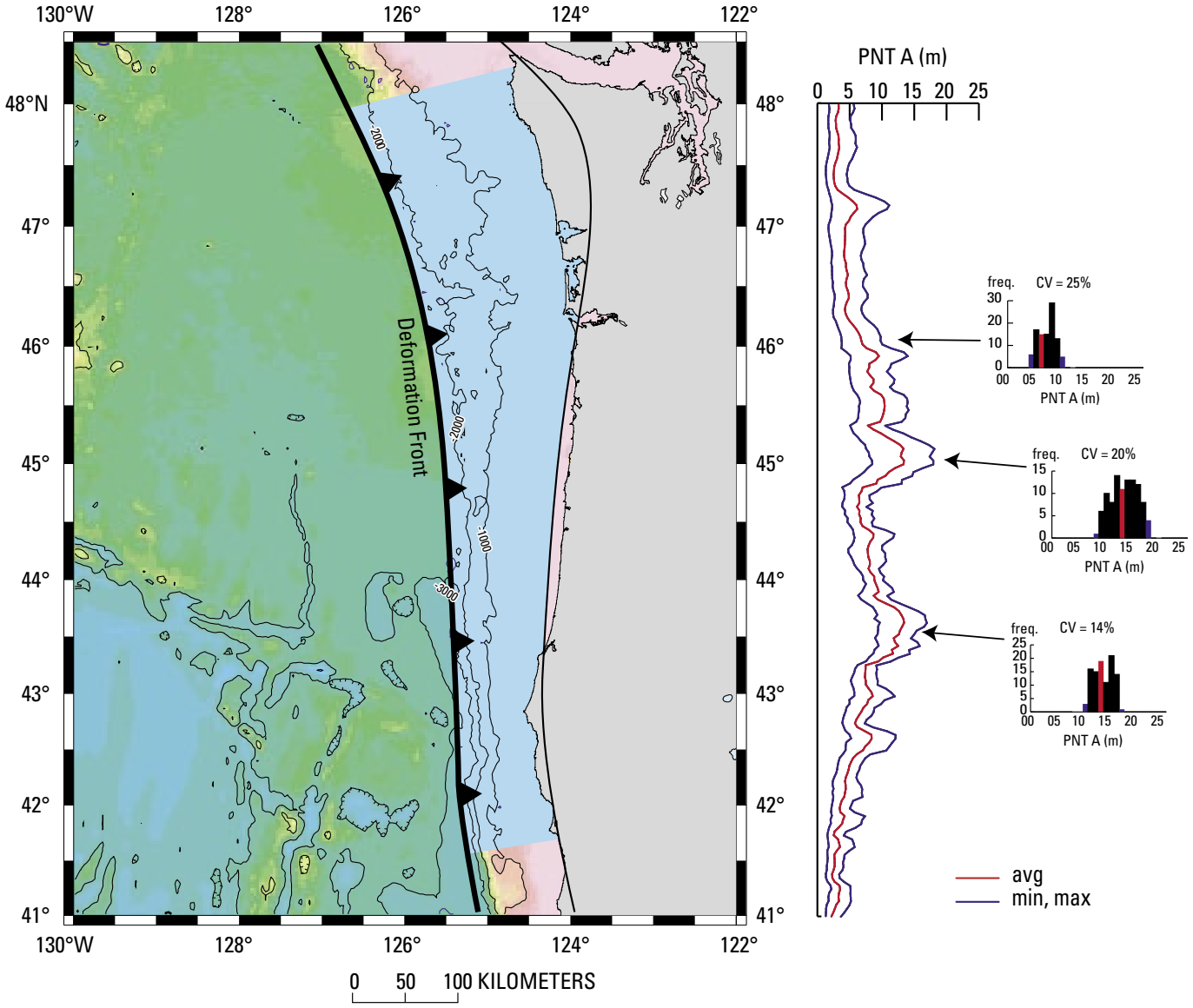

Figure 3. Alongshore distribution of peak nearshore tsunami amplitude (PNTA) using a geometry similar to the "Long-Wide" geometry of Satake and others (2003) and slip distributions from the stochastic source model (average slip 11.2-12.8 m with M_w = 9.0). Left: Rupture areas used for simulation are shown in light blue. Bathymetry in meters. Right: Average (red) and maximum and minimum values (blue) of PNTA using 100 slip distribution patterns. Histograms represent frequency of occurrence for PNTA bins of 1.0 m at three selected localities. CV is the coefficient of variation.

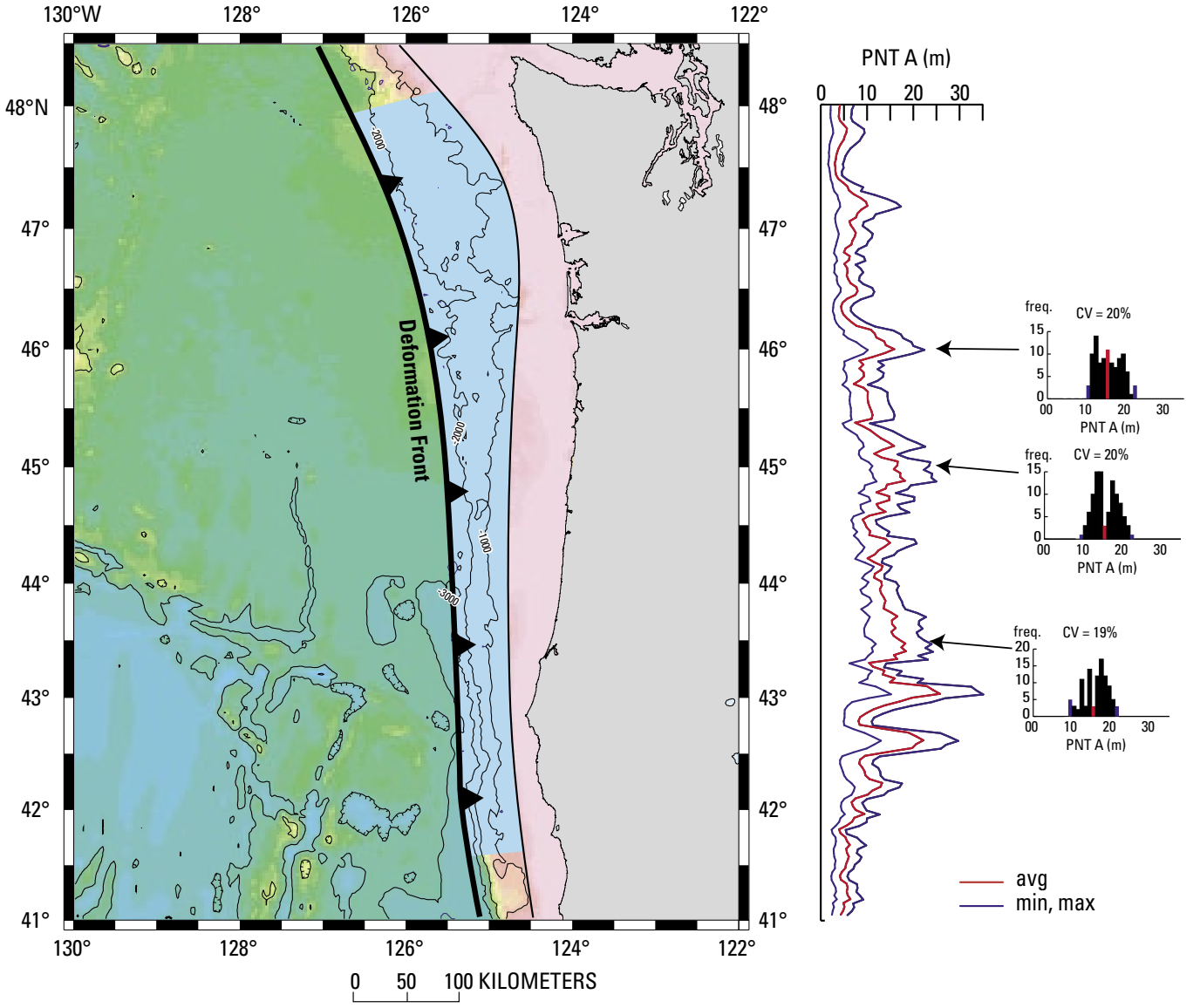

Figure 4. Alongshore distribution of peak nearshore tsunami amplitude (PNTA) using a geometry similar to the "Long-Narrow" geometry of Satake and others (2003) and slip distributions from the stochastic source model (average slip 12.5-14.5 m with M_w = 8.8-8.9). Left: Rupture areas used for simulation are shown in light blue. Bathymetry in meters. Right: Average (red) and maximum and minimum values (blue) of PNTA using 100 slip distribution patterns. Histograms represent frequency of occurrence for PNTA bins of 1.0 m at three selected localities. CV is the coefficient of variation.

(Frankel and others, 2002). Uncertainties in earthquake magnitude and geometry for interplate thrust earthquakes along the Cascadia subduction zone are incorporated into the probability calculations by defining six source scenarios: two possible characteristic magnitudes (M 9 and M 8.3) combined with three possible positions of the downdip edge of the rupture zone (Frankel and others, 2002). Similarly, for tsunami-hazard probability calculations, one should also include a splay fault scenario as in Geist and Yoshioka (1996) and Satake and others (2003). Uncertainty of the slip distribution is most likely an aleatory uncertainty, since it is essentially unpredictable and repeated occurrence of a particular earthquake (for example, a M 9 Cascadia event) will result in changes in PNTA related to changes in the slip distribution (fig. 4). Alternatively (though not consistent with the findings of Kelsey and others, 2002), if one were to consider Cascadia subduction-zone earthquakes as being characteristic sensu stricto (that is, slip distribution and rupture area are constant from earthquake to earthquake), then the uncertainty associated with the unknown slip distribution would be epistemic, since once the earthquake occurs, the slip distribution would be known (see Thought Experiment 2 in Anderson and Brune, 1999). Analysis of repeated earthquakes along subduction zones suggest, however, that slip distribution patterns vary from event to event (Thatcher, 1990; Boyd and others, 1995) and are best described as being a source of aleatory uncertainty.

Summary

Although probabilistic tsunami hazard analysis (PTHA) shares many similarities with probabilistic seismic hazard analysis (PSHA), there are several issues unique to tsunami generation and propagation that need to be resolved before routine calculations are performed. For example, tsunami generation is sensitive to the possibility of rupture on splay faults within the subduction zone such that a splay-fault scenario would have to be added as a separate branch to a logic tree, following the approach outlined by Frankel and others (2002). In addition, although there is little aleatory uncertainty associated with the propagation calculations, as there is with attenuation relations in PSHA, the variation in slip-distribution patterns has a significant effect on nearshore tsunami amplitudes and is itself a source of aleatory uncertainty. Using rupture geometries specified by Satake and others (2003) for a M ~ 9 earthquake, predicted offshore tsunami amplitudes are similar to results from previous studies for a wide rupture, but slightly larger than previously predicted for a narrow rupture. For a given rupture geometry and seismic moment, the coefficient of variation for offshore tsunami amplitudes typically ranges between 15 and 25 percent. The overriding uncertainty for these calculations, however, is the magnitude and attendant first-order source parameters (area, average slip, shear modulus) of a future Cascadia earthquake.

Another issue to be decided is what tsunami hydrodynamic parameter would be mapped under PTHA. Presently, tsunami inundation maps show the inundation limit for different source scenarios. In contrast, the tsunami parameter analogous to exceedance probabilities of peak ground motion or response spectral acceleration in PSHA and of concern to engineers is most likely the exceedance probability of peak current velocity over the region of inundation. For example, one could present a PTHA map along the Cascadia coastline for inundation velocities with, for example, a 2-percent probability of exceedance in the next 50 years. Current velocities, however, are also most sensitive to errors in nearshore bathymetry and topography. Wave-height exceedence probabilities such as calculated by Ward and Asphaug (2000) are more tractable, given current technology and available bathymetric/topographic data in the coastal zone. Though the resolution of issues related to PTHA may be difficult, the analysis will incorporate scientifically defensible estimates of uncertainties and provide an improved technique with which to evaluate tsunami hazards.

Acknowledgments

Generic Mapping Tools software from Wessel and Smith (1998) was used to produce the maps. The author is grateful to Tom Brocher and Hal Mofjeld for suggesting important changes to this paper.

References

Abe, K., and Ishii, H., 1980, Propagation of tsunami on a linear slope between two flat regions; Part II reflection and transmission: Journal of Physics of the Earth, v. 28, p. 543-552.

Adams, J., 1996, Great earthquakes recorded by turbidites off the Oregon-Washington coast: U.S. Geological Survey Professional Paper 1560, v. 1, p. 147-158.

Aki, K., 1967, Scaling law of seismic spectrum: Journal of Geophysical Research, v. 72, p. 1212-1231.

Anderson, J. G., and Brune, J. N., 1999, Probabilistic seismic hazard analysis without the ergodic assumption: Seismological Research Letters, v. 70, p. 19-28.

Andrews, D. J., 1980, A stochastic fault model 1; static case: Journal of Geophysical Research, v. 85, p. 3867-3877.

Antunes do Carmo, J. S., and Seabra-Santos, F. J., 1996, On breaking waves and wave-current interaction in shallow water; a 2DH finite element model: International Journal for Numerical Methods in Fluids, v. 22, p. 429-444.

Aochi, H., Fukuyama, E., and Matsu'ura, M., 2000, Selectivity of spontaneous rupture propagation on a branched fault: Geophysical Research Letters, v. 27, p. 3635-3638.

Atwater, B. F., 1987, Evidence for great Holocene earthquakes along the outer coast of Washington State: Science, v. 236, p. 942-944.

Atwater, B. F., 1992, Geologic evidence for earthquakes during the past 2000 years along the Copalis River, southern coastal Washington: Journal of Geophysical Research, v. 97, p. 1901-1919.

Atwater, B. F., and Hemphill-Haley, E., 1997, Recurrence intervals for great earthquakes of the past 3,500 years at northeastern Willapa Bay, Washington: U.S. Geological Survey Professional Paper 1576, 108 p.

Beck, S. L., and Ruff, L. J., 1989, Great earthquakes and subduction along the Peru trench: Physics of the Earth and Planetary Interiors, v. 57, p. 199-224.

Bilek, S. L., and Lay, T., 2002, Tsunami earthquakes possibly widespread manifestations of frictional conditional stability: Geophysical Research Letters, v. 29, p. 18-1 to 18-4.

Blumberg, A. F., and Mellor, G. L., 1987, A description of a three-dimensional coastal ocean circulation model, *in* Heaps, N. S., ed., Coastal and Estuarine Sciences, v. 4; three-dimensional coastal ocean models: Washington D.C., American Geophysical Union, p. 1-16.

Boyd, T. M., Engdahl, E. R., and Spence, W., 1995, Seismic cycles along the Aleutian arc; analysis of seismicity from 1957 through 1991: Journal of Geophysical Research, v. 100, p. 621-644.

Carrier, G. F., 1971, The dynamics of tsunamis, *in* Reid, W. H., ed., Mathematical problems in the geophysical sciences 1; geophysical fluid dynamics: Providence, Rhode Island, American Mathematical Society, Lectures in Applied Mathematics, v. 13, p. 157-187.

Carrier, G. F., 1995, On-shelf tsunami generation and coastal propagation, *in* Tsuchiya, Y., and Shuto, N., eds., Tsunami; progress in prediction, disaster prevention and warning: Dordrecht, The Netherlands, Kluwer Academic Publishers, p. 1-20.

Carrier, G. F., and Greenspan, H. P., 1958, Water waves of finite amplitude on a sloping beach: Journal of Fluid Mechanics, v. 17, p. 97-109.

Carrier, G. F., and Noiseux, C. F., 1983, The reflection of obliquely incident tsunamis: Journal of Fluid Mechanics, v. 133, p. 147-160.

Cornell, C. A., 1968, Engineering seismic risk analysis: Bulletin of the Seismological Society of America, v. 58, p. 1583-1606.

Cramer, C., Petersen, M. D., and Reichle, M. S., 1996, A Monte Carlo approach in estimating uncertainty for a seismic hazard assessment of Los Angeles, Ventura, and Orange Counties, California: Bulletin of the Seismological Society of America, v. 86, p. 1681-1691.

Cummins, P. R., and Kaneda, Y., 2000, Possible splay fault slip during the 1946 Nankai earthquakes: Geophysical Research Letters, v. 27, p. 2725-2728.

Dmowska, R. and Kostrov, B. V., 1973, A shearing crack in a semi-space under plane strain conditions: Archives of Mechanics, v. 25, p. 421-440.

Dragert, H., Hyndman, R. D., Rogers, G. C., and Wang, K., 1994, Current deformation and the width of the seismogenic zone of the northern Cascadia subduction thrust: Journal of Geophysical Research, v. 99, p. 653-668.

Dragert, H., Wang, K., and James, T. S., 2001, A silent slip event on the deeper Cascadia subduction interface: Science, v. 292, p. 1525-1528.

Ellsworth, W. L., Matthews, M. V., Nadeau, R. M., Nishenko, S. P., Reasenberg, P. A., and Simpson, R. W., 1999, A physically-based earthquake recurrence model for estimation of long-term earthquake probabilities: U. S. Geological Survey Open-File Report 99-522, 22 p.

Flück, P., Hyndman, R. D., and Wang, K., 1997, Three-dimensional dislocation model for great earthquake of the Cascadia subduction zone: Journal of Geophysical Research, v. 102, p. 20539-20550.

Frankel, A., 1991, High-frequency spectral falloff of earthquakes, fractal dimension of complex rupture, b value, and the scaling of strength on faults: Journal of Geophysical Research, v. 96, p. 6291-6302.

Frankel, A., Mueller, C., Barnhard, T., Perkins, D., Leyendecker, E. V., Dickman, N., Hanson, S., and Hopper, M., 1996, National seismic-hazard maps; documentation June 1996: U.S. Geological Survey Open-File Report 96-532, 110 p.

Frankel, A. D., Petersen, M. D., Mueller, C. S., Haller, K. M., Wheeler, R. L., Leyendecker, E. V., Wesson, R. L., Harmsen, S. C., Cramer, C. H., Perkins, D. M., and Rukstales, K. S., 2002, Documentation for the 2002 update of the national seismic hazard maps: U.S. Geological Survey Open-File Report 02-242, 33 p.

Freund, L. B., and Barnett, D. M., 1976, A two-dimensional analysis of surface deformation due to dip-slip faulting: Bulletin of the Seismological Society of America, v. 66, p. 667-675.

Fujima, K., Dozono, R., and Shigemura, T., 2000, Generation and propagation of tsunami accompanying edge waves on a uniform sloping shelf: Coastal Engineering Journal, v. 42, p. 211-236.

Fukao, Y., 1979, Tsunami earthquakes and subduction processes near deep-sea trenches: Journal of Geophysical Research, v. 84, p. 2303-2314.

Geist, E. L., 1999, Local tsunamis and earthquake source parameters, *in* Dmowska, R., and Saltzman, B., eds., Tsunamigenic earthquakes and their consequences: Advances in Geophysics, v. 39, p. 117-209.

Geist, E. L., 2002, Complex earthquake rupture and local tsunamis: Journal of Geophysical Research, v. 107, p. ESE 2-1 to ESE 2-16, doi; 10.1029/2000JB000139.

Geist, E. L., and Bilek, S. L., 2001, Effect of depth-dependent shear modulus on tsunami generation along subduction zones: Geophysical Research Letters, v. 28, p. 1315-1318.

Geist, E. L., and Dmowska, R., 1999, Local tsunamis and distributed slip at the source: Pure and Applied Geophysics, v. 154, p. 485-512.

Geist, E. L., and Yoshioka, S., 1996, Source parameters controlling the generation and propagation of potential local tsunamis along the Cascadia margin: Natural Hazards, v. 13, p. 151-177.

Geller, R. J., 1976, Scaling relations for earthquake source parameters and magnitudes: Bulletin of the Seismological Society of America, v. 66, p. 1501-1523.

Goldfinger, C. , Nelson, C. H., Johnson, J. E., and The Shipboard Scientific Party, 2003, Holocene earthquake records from the Cascadia subduction zone and northern San Andreas Fault based on precise dating of offshore turbidites: Annual Review of Earth and Planetary Sciences, v. 31, p. 555-577.

González, F. I., Satake, K., Boss, F., and Mofjeld, H. O., 1995, Edge wave and non-trapped modes of the 25 April 1992 Cape Mendocino tsunami: Pure and Applied Geophysics, v. 144, p. 409-426.

Hanks, T. C., 1979, *b* values and $\omega^{-\gamma}$ seismic source models; implications for tectonic stress variations along active crustal fault zones and the estimation of high-frequency strong ground motion: Journal of Geophysical Research, v. 84, p. 2235-2242.

Hartzell, S. H., and Heaton, T. H., 1985, Teleseismic time functions for large, shallow, subduction zone earthquakes: Bulletin of the Seismological Society of America, v. 75, p. 965-1004.

Heaton, T. H., and Hartzell, S. H., 1986, Source characteristics of hypothetical subduction earthquakes in the northwestern United States: Bulletin of the Seismological Society of America, v. 76, p. 675-708.

Heaton, T. H., and Hartzell, S. H., 1989, Estimation of strong ground motions for hypothetical earthquakes on the Cascadia subduction zone, Pacific Northwest: Pure and Applied Geophysics, v. 129, p. 131-201.

Heaton, T. H., and Kanamori, H., 1984, Seismic potential associated with subduction in the northwestern United States: Bulletin of the Seismological Society of America, v. 74, p. 933-941.

Hebenstreit, G. T., and Murty, T. S., 1989, Tsunami amplitudes from local earthquakes in the Pacific Northwest region of North America, part 1—the outer coast: Marine Geodesy, v. 13, p. 101-146.

Herrero, A. and Bernard, P., 1994, A kinematic self-similar rupture process for earthquakes: Bulletin of the Seismological Society of America, v. 84, p. 1216-1228.

Houston, J. R., Carver, R. D., and Markle, D. G., 1977, Tsunami-wave elevation frequency of occurrence for the Hawaiian Islands: U.S. Army Corps of Engineers Waterways Experiment Station Technical Report H-66-16, 109 p.

Huang, J., and Turcotte, D. L., 1988, Fractal distributions of stress and strength and variations of b-value: Earth and Planetary Science Letters, v. 91, p. 223-230.

Hyndman, R. D., and Wang, K., 1995, The rupture zone of Cascadia great earthquakes from current deformation and the thermal regime: Journal of Geophysical Research, v. 100, p. 22133-22154.

Ihmlé, P. F., 1996, Monte Carlo slip inversion in the frequency domain; application to the 1992 Nicaragua slow earthquake: Geophysical Research Letters, v. 23, p. 913-916.

Imamura, F., Gica, E., Takahashi, T., and Shuto, N., 1995, Numerical simulation of the 1992 Flores tsunami; interpretation of tsunami phenomena in northeastern Flores Island and damage at Babi Island: Pure and Applied Geophysics, v. 144, p. 555-568.

Ishii, H., and Abe, K., 1980, Propagation of tsunami on a linear slope between two flat regions, part I—edge wave: Journal of Physics of the Earth, v. 28, p. 531-541.

Jeyakumaran, M., and Keer, L. M., 1994, Curved slip zones in an elastic half-plane: Bulletin of the Seismological Society of America, v. 84, p. 1903-1915.

Johnsgard, H., and Pedersen, G., 1997, A numerical model for three-dimensional run-up: International Journal for Numerical Methods in Fluids, v. 24, p. 913-931.

Kajiura, K., 1963, The leading wave of a tsunami: Bulletin of the Earthquake Research Institute, University of Tokyo, v. 41, p. 535-571.

Kame, N., Rice, J.R., and Dmowska, R., 2003, Effects of prestress state and rupture velocity on dynamic fault branching: Journal of Geophysical Research, v. 108, no. B5, p. ESE 13-1 to 13-21.

Kanamori, H., 1972, Mechanism of tsunami earthquakes: Physics of the Earth Planetary Interiors, v. 6, p. 346-359.

Kanamori, H., 1981, The nature of seismicity patterns before large earthquakes, *in* Simpson, D. W., and Richards, P. G., eds., Earthquake prediction; an international review: American Geophysical Union, Maurice Ewing Series 4, p. 1-19.

Kanamori, H., and Anderson, D. L., 1975, Theoretical basis of some empirical relations in seismology: Bulletin of the Seismological Society of America, v. 65, p. 1073-1095.

Kanamori, H., and Kikuchi, M., 1993, The 1992 Nicaragua earthquake; a slow tsunami earthquake associated with subducted sediments: Nature, v. 361, p. 714-716.

Kelsey, H. M., Witter, R. C., and Hemphill-Haley, E., 2002, Plate-boundary earthquakes and tsunamis of the past 5500 yr, Sixes River estuary, southern Oregon: Geological Society of America Bulletin, v. 114, p. 298-314.

Koshimura, S., Imamura, F., and Shuto, N., 1999, Propagation of obliquely incident tsunamis on a slope, part I—amplification of tsunamis on a continental slope: Coastal Engineering Journal, v. 41, p. 151-164.

Leonard, L. J., Hyndman, R. D., and Mazzotti, S., 2004, Coseismic subsidence in the 1700 Great Cascadia earthquake: Coastal estimates versus elastic dislocation models: Geological Society of America Bulletin, v. 116, p. 655-670.

Lin, I. C., and Tung, C. C., 1982, A preliminary investigation of tsunami hazard: Bulletin of the Seismological Society of America, v. 72, p. 2323-2337.

Ludwin, R. S., Weaver, C. S., and Crosson, R. S., 1991, Seismicity of Washington and Oregon, *in* Slemmons, D. B., Engdahl, E. R., Zoback, M. D., and Blackwell, D. D., eds., Neotectonics of North America: Boulder, Colorado, Geological Society of America, Decade Map Volume 1, p. 77-98.

MacKay, M. E., Moore, G. F., Cochrane, G. R., Moore, J. C., and Kulm, L. D., 1992, Landward vergence and oblique structural trends in the Oregon margin accretionary prism; implications and effect on fluid flow: Earth and Planetary Science Letters, v. 109, p. 477-491.

Madariaga, R., Olsen, K., and Archuleta, R., 1998, Modeling dynamic rupture in a 3D earthquake fault model: Bulletin of the Seismological Society of America, v. 88, p. 1182-1197.

Mazzotti, S., Le Pichon, X., Henry, P., and Miyazaki, S., 2000, Full interseismic locking of the Nankai and Japan-west Kurile subduction zones; an analysis of uniform elastic strain accumulation in Japan constrained by permanent GPS: Journal of Geophysical Research, v. 105, p. 13159-13177.

Mei, C. C., 1983, The applied dynamics of ocean surface waves: New York, John Wiley and Sons, 740 p.

Mellor, G. L., and Yamada, T., 1974, A hierarchy of turbulence closure models for planetary boundary layers: Journal of Atmospheric Sciences, v. 31, p. 1791-1896.

Mitchell, C. E., Vincent, P., Weldon, R. J., II, and Richards, M. A., 1994, Present-day vertical deformation of the Cascadia Margin, Pacific Northwest, United States: Journal of Geophysical Research, v. 99, p. 12257-12277.

Mofjeld, H.O., Foreman, M. G. G., and Ruffman, A., 1997, West Coast tides during Cascadia subduction zone tsunamis: Geophysical Research Letters, v. 24, p. 2215-2218.

Mofjeld, H. O., González, F. I., and Newman, J. C., 1999, Tsunami prediction in U.S. coastal regions: Coastal and Estuarine Studies, v. 56, p. 353-375.

National Research Council, 1988, Probabilistic seismic hazard analysis: Washington D.C., National Academy Press, 97 p.

Ng, M. K.-F., LeBlond, P. H., and Murty, T. S., 1990, Simulation of tsunamis from great earthquakes on the Cascadia subduction zone: Science, v. 250, p. 1248-1251.

Nielsen, S. B., Carlson, J. M., and Olsen, K. B., 2000, Influence of friction and fault geometry on earthquake rupture: Journal of Geophysical Research, v. 105, p. 6069-6088.

Okada, Y., 1985, Surface deformation due to shear and tensile faults in a half-space: Bulletin of the Seismological Society of America, v. 75, p. 1135-1154.

Oleskevich, D. A., Hyndman, R. D., and Wang, K., 1999, The updip and downdip limits to great subduction earthquakes; thermal and structural models of Cascadia, south Alaska, SW Japan, and Chile: Journal of Geophysical Research, v. 104, p. 14965-14991.

Oppenheimer, D., Beroza, G., Carver, G., Dengler, L., Eaton, L., Gee, L., González, F., Jayko, A., Li, W. H., Lisowski, M., Magee, M., Marshall, G., Murray, M., McPherson, R., Romanowicz, B., Satake, K., Simpson, R., Somerville, P., Stein, R., and Valentine, D., 1993, The Cape Mendocino, California, earthquake of April 1992; subduction at the triple junction: Science, v. 261, p. 433-438.

Panel on Seismic Hazard Evaluation, 1997, Review of "Recommendations for Probabilistic Seismic Hazard Analysis; Guidance on Uncertainty and Use of Experts": Washington D.C., National Academy Press, 73 p.

Pérez, O. J., and Scholz, C. H., 1997, Long-term seismic behavior of the focal and adjacent regions of great earthquakes during the time between two successive shocks: Journal of Geophysical Research, v. 102, p. 8203-8216.

Piatanesi, A., Tinti, S., and Gavagni, I., 1996, The slip distribution of the 1992 Nicaragua earthquake from tsunami run-up data: Geophysical Research Letters, v. 23, p. 37-40.

Plafker, G., 1965, Tectonic deformation associated with the 1964 Alaska earthquake: Science, v. 148, p. 1675-1687.

Polet, J., and Kanamori, H., 2000, Shallow subduction zone earthquakes and their tsunamigenic potential: Geophysical Journal International, v. 142, p. 684-702.

Preuss, J., and Hebenstreit, G. T., 1998, Integrated tsunami-hazard assessment for a coastal community, Grays Harbor, Washington: U.S. Geological Survey Professional Paper 1560, v. 2, p. 517-536.

Priest, G. R., Myers, E., Baptista, A. M., Fleuck, P., Wang, K., Kamphaus, R. A., and Peterson, C. D., 1997, Cascadia subduction zone tsunamis; hazard mapping at Yaquina Bay, Oregon: Oregon Department of Geology and Mineral Industries, Open-File Report O-97-34, 144 p.

Priest, G. R., Myers, E., Baptista, A. M., Fleuck, P., Wang, K., and Peterson, C. D., 2000, Source simulation for tsunamis; lessons learned from fault rupture modeling of the Cascadia subduction zone, North America: Science of Tsunami Hazards, v. 18, p. 77-105.

Rikitake, T., and Aida, I., 1988, Tsunami hazard probability in Japan: Bulletin of the Seismological Society of America, v. 78, p. 1268-1278.

Rogers, A. M, Walsh, T. J., Kockelman, W. J., and Priest, G. R., 1996, Earthquake hazards in the Pacific Northwest—an overview: U.S. Geological Survey Professional Paper 1560, v. 1, p. 1-67.

Romanowicz, B., and Rundle, J., 1993, On scaling relations for large earthquakes: Bulletin of the Seismological Society of America, v. 83, p. 1294-1297.

Rudnicki, J. W., and Wu, M., 1995, Mechanics of dip-slip faulting in an elastic half-space: Journal of Geophysical Research, v. 100, p. 22173-22186.

Rybicki, K., 1986, Dislocations and their geophysical application, *in* Teisseyre, R., ed., Continuum theories in solid earth physics: Warsaw, PWN-Polish Scientific Publishers, p. 18-186.

Satake, K., 2002, Tsunamis, *in* Lee, W.H.K., Kanamori, H., Jennings, P.C., and Kisslinger, C., eds., International handbook of earthquake and engineering seismology, chapter 28: International Association of Seismology and Physics of the Earth's Interior (IASPEI), p. 437-451.

Satake, K., and Tanioka, Y., 1995, Tsunami generation of the 1993 Hokkaido Nansei-Oki earthquake: Pure and Applied Geophysics, v. 144, p. 803-821.

Satake, K., and Tanioka, Y., 1999, Sources of tsunami and tsunamigenic earthquakes in subduction zones: Pure and Applied Geophysics, v. 154, p. 467-483.

Satake, K., Shimazaki, K., Tsuji, Y., and Ueda, K., 1996, Time and size of a giant earthquake in Cascadia inferred from Japanese tsunami record of January 1700: Nature, v. 379, p. 246-249.

Satake, K., Wang, K., and Atwater, B.F., 2003, Fault slip and seismic moment of the 1700 Cascadia earthquake inferred from Japanese tsunami descriptions: Journal of Geophysical Research, v. 108, p. ESE 7-1 to 7-17; doi: 10.1029/2003JB002521.

Sato, S., 1996, Numerical simulation of the propagation of the 1993 southwest Hokkaido earthquake tsunami around Okushiri Island: Science of Tsunami Hazards, v. 14, p. 119-134.

Savage, J. C., Lisowski, M., and Prescott, W. H., 1991, Strain accumulation in western Washington: Journal of Geophysical Research, v. 96, p. 14493-14507.

Scholz, C. H., 1990, The mechanics of earthquakes and faulting: Cambridge, England, Cambridge University Press, 439 p.

Scholz, C. H., 1994, A reappraisal of large earthquake scaling: Bulletin of the Seismological Society of America, v. 84, p. 215-218.

Senior Seismic Hazard Analysis Committee, 1997, Recommendations for probabilistic seismic hazard analysis; guidance on uncertainty and use of experts: Washington D.C., U.S. Nuclear Regulatory Commission, NUREG/CR-6372, 256 p.

Shibata, M., 1983, One-dimensional dispersive deformation of tsunami with typical initial profiles on continental topographies, *in* Iida, J., and Iwasaki, T., eds., Tsunamis; their science and engineering: Tokyo, Terra Science Publication Company, p. 241-250.

Shuto, N., 1991, Numerical simulation of tsunamis—its present and near future: Natural Hazards, v. 4, p. 171-191.

Steketee, J. A., 1958, On Volterra's dislocations in a semi-infinite medium: Canadian Journal of Physics, v. 36, p. 192-205.

Tanioka, Y., and Satake, K., 1996, Tsunami generation by horizontal displacement of ocean bottom: Geophysical Research Letters, v. 23, p. 861-864.

Thatcher, W., 1990, Order and diversity in the modes of circum-Pacific earthquake recurrence: Journal of Geophysical Research, v. 95, p. 2609-2623.

Tichelaar, B. W., and Ruff, L. J., 1993, Depth of seismic coupling along subduction zones: Journal of Geophysical Research, v. 98, p. 2017-2037.

Titov, V. V., and Synolakis, C. E., 1998, Numerical modeling of tidal wave runup: Journal of Waterways, Port, Coastal and Ocean Engineering, v. 124, p. 157-171.

Toro, G. W., Abrahamson, N. A., and Schneider, J. F., 1997, Model of strong ground motions from earthquakes in central and eastern North America; best estimates and uncertainties: Seismological Research Letters, v. 68, p. 41-57.

Tsai, C. P., 1997, Slip, stress drop and ground motion of earthquakes; a view from the perspective of fractional Brownian motion: Pure and Applied Geophysics, v. 149, p. 689-706.

Walsh, T. J., Caruthers, C. G, Heinitz, A. C., Myers, E. P., III, Baptista, A. M., Erdakos, G. B., and Kamphaus, R. A., 2000, Tsunami hazard map of the southern Washington coast; modeled tsunami inundation from a Cascadia subduction zone earthquake: Washington Division of Geology and Earth Resources Geologic Map GM-49, scale 1:100,000.

Wang, K., Wells, R.E., Mazzotti, S., Hyndman, R.D., and Sagiya, T., 2003, A revised dislocation model of the interseismic deformation of the Cascadia subduction zone: Journal of Geophysical Research, v. 108, p. ETG 9-1 to ETG9-13; doi:10.1029/2001JB001703.

Ward, S. N., 1980, Relationships of tsunami generation and an earthquake source: Journal of Physics of the Earth, v. 28, p. 441-474.

Ward, S. N., 1994, A multidisciplinary approach to seismic hazard in southern California: Bulletin of the Seismological Society of America, v. 85, p. 1293-1309.

Ward, S. N., 2000, Tsunamis, *in* Encyclopedia of Physical Science and Technology: San Diego, Academic Press, p. 175-191.

Ward, S. N., 2001, Landslide tsunami: Journal of Geophysical Research, v. 106, p. 11201-11215.

Ward, S. N., and Asphaug, E., 2000, Asteroid impact tsunami; a probabilistic hazard assessment: Icarus, v. 145, p. 64-78.

Wells, D. L., and Coppersmith, K. J., 1994, New empirical relationships among magnitude, rupture length, rupture width, rupture area, and surface displacement: Bulletin of the Seismological Society of America, v. 84, p. 974-1002.

Wesnousky, S. G., 1994, The Gutenberg-Richter or characteristic earthquake distribution, which is it?: Bulletin of the Seismological Society of America, v. 84, p. 1940-1959.

Wessel, P., and Smith, W. H. F, 1998, New, improved version of Generic Mapping Tools released: Eos, Transactions of the American Geophysical Union, v. 79, p. 579.

Whitmore, P. M., 1993, Expected tsunami amplitudes and currents along the North American coast for Cascadia subduction zone earthquakes: Natural Hazards, v. 8, p. 59-73.

Witter, R. C., Kelsey, H. M., and Hemphill-Haley, E., 2003, Great Cascadia earthquakes and tsunamis of the past 6700 years, Coquille River estuary, southern coastal Oregon: Geological Society of America Bulletin, v. 115, p. 1289-1306.

Wyss, M., 1979, Estimating maximum expectable magnitude of earthquakes from fault dimensions: Geology, v. 7, p. 336-340.

Zhang, Z., and Schwartz, S. Y., 1992, Depth distribution of moment release in underthrusting earthquakes at subduction zones: Journal of Geophysical Research, v. 97, p. 537-544.

Zheng, G., and Rice, J. R., 1998, Conditions under which velocity-weakening friction allows a self-healing versus a cracklike mode of rupture: Bulletin of the Seismological Society of America, v. 88, p. 1466-1483.

.